

# Estimation of Fibrous Aerosol Deposition in Upper Bronchi Based on Experimental Data with Model Bifurcation

Toshihiko MYOJO\* and Mitsutoshi TAKAYA

National Institute of Industrial Health, Nagao, Tama-ku, Kawasaki, 214-8585, Japan

Received October 31, 2000 and accepted January 23, 2001

**Abstract:** Lung deposition of fibrous aerosol was studied by using a model of the lung bifurcation with dimensions based on the symmetric model A of Weibel. The fibrous aerosols were introduced to the model under steady inspiratory flow conditions. Glass fibers depositing in the daughter tubes and these escaping from them were observed under a scanning electron microscope (SEM). The deposited fractions were calculated for each length and diameter using a bivariate lognormal distribution. In this study the authors propose empirical equations to estimate total deposited fractions of fibrous aerosol at upper bronchi. The dimensionless relationship among deposited fractions  $F_d$ , Stokes number  $St$  for randomly-oriented fibers and interception parameter  $I$  were used to estimate the deposited fraction at arbitrary position in the upper bronchi. The calculation procedure for  $F_d(St, I)$  consists of two steps: the determination of the four deposited fractions,  $F_{d_n}$  for each  $I_n$  ( $n=1\sim 4$ ) followed by interpolation or extrapolation from  $F_{d_n}$  to find the deposited fraction  $F_d$  at a given  $I$ . With this procedure, it is possible to determine the deposited fraction  $F_d$  in the range of  $2 \times 10^{-3} < St < 5 \times 10^{-2}$  and  $5 \times 10^{-4} < I < 5 \times 10^{-2}$ . Penetration from the trachea to the 10th generation of lung bifurcation was calculated for several cases of fiber diameter, length and flow rate. In the case corresponding to an inspiration of 500 cm<sup>3</sup> air at a constant rate for 2 s, more than half of the fibers with a length of 100  $\mu\text{m}$  and diameter of 3  $\mu\text{m}$  are deposited at upper bronchi but more than 90% of fibers of the same length and 1  $\mu\text{m}$  in diameter pass through the region.

**Key words:** Fiber, Asbestos, Inhalation, Lung

## Nomenclature

CML	count medium length, $CML = \exp(\mu_L)$	$B = (\ln L_f - \mu_L)/\beta_L$	
CMD	count medium diameter, $CMD = \exp(\mu_D)$	$F_d(D, L_1, L_2)$	deposited fraction averaged over $D$ to $D+\Delta D$ diameter and $L_1$ to $L_2$ length fibers
Df	fiber diameter	$F_d(L_1, L_2)$	deposited fraction averaged over $L_1$ to $L_2$ length fibers
$F(D_f, L_1, L_2)$	distribution function defined by equation (4)	$I$	interception parameter
$f(L_f, D_f)$	probability density function of bivariate lognormal distribution	$L_f$	fiber length
	$f(L_f, D_f) =$	$L_1$ and $L_2$	measured fiber length range
	$\frac{1}{2\pi\beta_L\beta_D(1-\tau^2)^{0.5}L_fD_f} \exp\left[-\frac{A^2+B^2-2\tau AB}{2(1-\tau^2)}\right]$	$m$	generation of lung bifurcation
	$A = (\ln D_f - \mu_D)/\beta_D$	$P$	penetration of fibrous aerosol at each bifurcation
		$R$	radius of airway
		$St$	Stokes number for randomly-oriented fibers
		$U$	mean air velocity in air way

\*To whom correspondence should be addressed.

$\beta_L, \beta_D$	square root of variance of the natural logarithms of Lf and Df
$\beta_{LD}$	co-variance of the natural logarithms of Lf and Df
$\eta$	viscosity of air
$\lambda$	angle between initial and final direction of air stream
$\mu_L, \mu_D$	arithmetic mean of the natural logarithms of Lf and Df
$\rho$	density of aerosol particles or fibers
$\sigma_g$	geometric standard deviation $\sigma_{g_L} = \exp(\beta_L)$
$\tau$	correlation between $\ln Lf$ and $\ln Df$ $\tau = \beta_{LD}/\beta_L \cdot \beta_D$
Subscript	
D	diameter
L	length

## Introduction

It is important to determine the initially deposited fractions of fibrous aerosols in the human respiratory system because lung disease is caused in part by the inability of the lung to remove the deposited fibers effectively. Beekman<sup>1</sup>, Harris and Fraser<sup>2</sup>, Harris and Timbrell<sup>3</sup>, Yu *et al.*<sup>4-7</sup>, Cai and Yu<sup>8</sup>, Asgharian and Yu<sup>9, 10</sup>, Chen and Yu<sup>11</sup>, Ding *et al.*<sup>12</sup> and Dai and Yu<sup>13</sup> proposed theoretical equations to estimate the deposited fraction in each respiratory compartment and/or total fraction of fibrous aerosols.

There are many inhalation experiments performed on laboratory animals. However, there are only a small number of experimental works on the deposition process of fibrous aerosols in airways with size-controlled fibrous aerosols<sup>14-16</sup> because it was difficult to generate and measure fibrous aerosols compared to compact aerosols, especially the lack of appropriate monodisperse fibrous aerosols in terms of both length and diameter. Therefore, no empirical equations to estimate the deposited fraction in lung bronchi have been proposed on the basis of measured data.

Myojo<sup>17-20</sup> previously observed deposited fractions of fibrous aerosols and presented profiles of deposition velocity on a simplified model of bifurcating tubes. The dimensions of the model bifurcation were based on the 3rd and 4th generation of Weibel's lung model A<sup>21</sup>, and a steady inspiratory flow of glass fiber aerosol was employed. Deposited fraction and deposition velocity for the fiber length range were obtained through the direct observation of fibers deposited on the model bifurcation. Bivariate lognormal distribution of fibrous aerosols has been assumed to characterize the length and the diameter of asbestos and man-

made mineral fibers<sup>22-24</sup>. Applying the bivariate lognormal distributions to deposited and non-deposited fibers, Myojo<sup>18-20</sup> determined the dependencies of deposited fractions on fiber diameter and fiber length, from the data on polydisperse fibrous aerosols.

In this study, to obtain the deposited fraction for wide range of fiber size, airway duct size and flow rate, additional data on the deposited fraction are measured with a model bifurcation between the 2nd and 3rd generations. Then the accumulated experimental data were reevaluated to find the functional dependence of the deposited fraction on Stokes number for randomly-oriented fibers and the interception parameter between fiber and airway duct. The authors propose empirical equations to estimate total deposited fractions of fibrous aerosol at upper bronchi.

## Experimental Methods

### *Experimental apparatus and procedure*

A general arrangement of the fibrous aerosol generator, the model bifurcation and the flow control units is essentially the same as that used in the previous work<sup>18, 19</sup>. A two-component fluidized aerosol generator was used to disperse fibers<sup>25</sup>. The fibers used in this study were glass fibers of a binderless HEPA filter (Toyo-roshi Co. Toyo GB100, Tokyo) sheared by means of a mill. The fibrous aerosols generated from the fluidized bed were led to an aerosol neutralizer (radioisotope <sup>85</sup>Kr) and plenum chamber. Aerosols were then passed through the model bifurcation at a steady inspiratory flow. Two model bifurcations, made of brass, corresponded approximately to the bifurcations between 2nd and 3rd or 3rd and 4th generations of Weibel's lung model A. The model dimensions are shown in Table 1. The fibers which did not deposit in the bifurcation were collected on Nuclepore filters (pore size 0.4  $\mu\text{m}$ ).

The flow rate in each daughter tube was 15.6  $\text{cm}^3 \text{s}^{-1}$  or 31.2  $\text{cm}^3 \text{s}^{-1}$ , corresponding to a breath of 500  $\text{cm}^3$  or 1000  $\text{cm}^3$ , respectively, inspired at a constant rate for 2 s.

In the 3rd run (see Table 1), an impactor was attached between the plenum chamber and bifurcation tubes to remove large fibers, as shown in the previous paper<sup>19</sup>. Further, in this work, a series consisting of an impactor (nozzle diameter; 6 mm) and a virtual impactor (nozzle diameter; 4 mm) were attached between the plenum chamber and bifurcation tubes to eliminate both small and large fibers. The flow rate through the both nozzles was 400  $\text{cm}^3 \text{s}^{-1}$ . These impactors were designed to provide compact glass particles ( $\rho=2.5 \text{ g cm}^{-3}$ ) between 1.7 and 2.1  $\mu\text{m}$  in diameter.

**Table 1. Experimental Condition**

Aerosol				
Material:	Glass fiber aerosol			
Generation method:	2-component fluidized bed			
Flow:	Steady inspiratory flow			
Model bifurcation				
Material:	Brass			
Position:	Vertical			
Branching angle:	45 degree			
Model	(I)	(II)		
Parent tube diameter:	0.8 (2nd)	0.6 cm (3rd)		
Daughter tube diameter:	0.6 (3rd)	0.4 cm (4th)		
Run No.	1	2	3	4
Flow rate	15.6 cm <sup>3</sup> s <sup>-1</sup>	31.2 cm <sup>3</sup> s <sup>-1</sup>	31.2 cm <sup>3</sup> s <sup>-1</sup>	31.2 cm <sup>3</sup> s <sup>-1</sup>
Impactor	No	No	Impactor	Impactor and Virtual Impactor
Model	II	II	II	I
Ref.	(19)	(19)	(19)	this work

#### Measurement of fibers and deposited fractions

The deposited fractions for each range of fiber length were determined as follows. The model bifurcation was disassembled and the observation part of the model bifurcation (indicated in Fig. 1) was mounted on the stage of the SEM (Hitachi, HS-2B). The wall surface of the daughter tube from carina to 4 mm or 6 mm in the axial direction and from carina to 90° in the circumferential direction (shaded area in Fig. 1) was directly observed under the SEM. In order to observe the curved tube wall from 0°

to 60° in circumferential direction, the SEM stage was tilted at 45°.

Serial micrographs of the deposited fibers were taken at low magnification (× 100) and the number and length of all fibers within the area were measured. As two kinds of bifurcation models were used in this study, we introduced the following interception parameter, in place of the fiber length.

$$I = Lf/2R \quad (1)$$

In the calculation of I, the geometric mean fiber length  $Lf = \sqrt{L_1 \cdot L_2}$  is used in the equation (1). In order to assign the same interception parameter to two model bifurcations, the fibers were divided into three length groups 13–26 μm, 26–52 μm and 52–104 μm for the 2nd and 3rd model and four length groups 10–20 μm, 20–40 μm, 40–80 μm and 70–110 μm for the 3rd and 4th model. Because there were only a small number of long fibers, the length ranges of 40–80 μm and 70–110 μm slightly overlapped.

More than 350 fibers collected on the Nuclepore filter were measured and the number concentrations of the aerosols were determined. From these data the deposited fractions  $F_d(L_1, L_2)$  of the bifurcation were calculated for the range of fibers with lengths from  $L_1$  to  $L_2$ .

At the same time, micrographs of the fibers were taken at three or four locations on the wall of the bifurcation tube (\* in Fig. 1) and on the Nuclepore filter (magnification × 500). From these photographs both the length and diameter of each fiber were measured to determine the means,

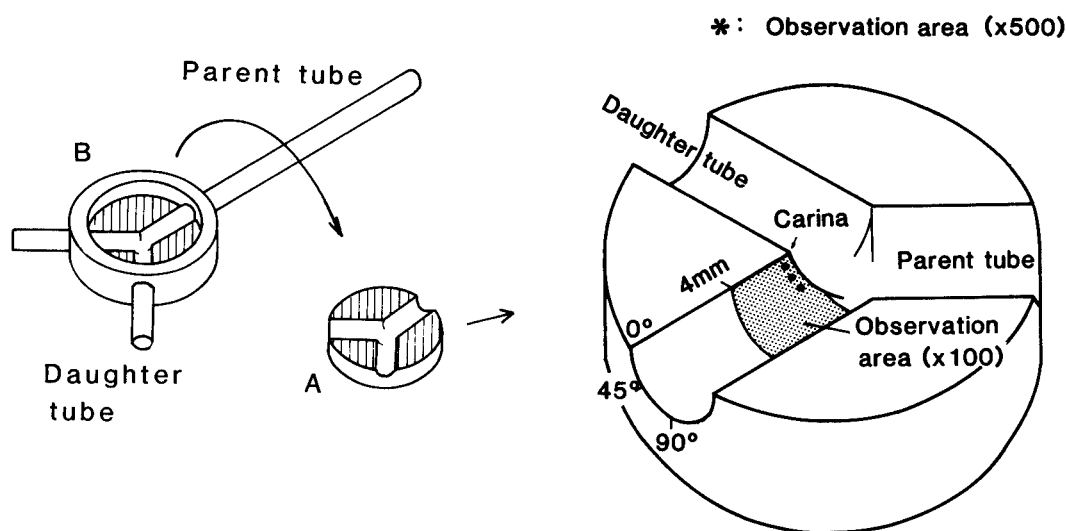


**Fig. 1. Observation part of the model bifurcation and its mounting methods on the SEM stage.**

After deposition of fibers, part A of the airway model is removed from part B and set in the SEM. Deposited fibers on shadow area of daughter tube wall were directly observed.

variances and correlation.

*Bivariate lognormal distributions and deposited fractions*

By expressing the joint length-diameter distribution of a fibrous aerosol by a bivariate lognormal distribution, deposited fractions for each size range of fiber length and diameter were determined. The deposition fraction for the length range from  $L_1$  to  $L_2$ , and for the diameter range  $D$  to  $D+\Delta D$ ,  $F_d(D, L_1, L_2)$  is given by

$$F_d(D, L_1, L_2) = F_d(L_1, L_2) \cdot K \tag{2}$$

where  $F_d(L_1, L_2)$  is the deposition fraction experimentally obtained by the method described in the previous section, and  $K$  is the factor defined by

$$K = \frac{F_{dep}(D + \Delta D, L_1, L_2) - F_{dep}(D, L_1, L_2)}{F_{in}(D + \Delta D, L_1, L_2) - F_{in}(D, L_1, L_2)} \tag{3}$$

$F_{dep}$  and  $F_{in}$  in equation (3) are the cumulative undersize distributions of deposited fibers and inlet fibers, respectively. If the bivariate lognormal distribution is applied,  $F$  is given by

$$F(D_f, L_1, L_2) = \frac{\int_{L_1}^{L_2} \int_{D_1}^{D_2} f(L, D) dLdD}{\int_{L_1}^{L_2} \int_{D_1}^{D_2} f(L, D) dLdD} \tag{4}$$

where  $f(L, D)$  is the probability function of the bivariate lognormal distribution. The probability function  $f(L, D)$

and additional statistical parameters are defined in the nomenclature. Equation (4) was solved by a numerical integration.

**Results and Discussion**

*Size distribution of fiber length and diameter*

The parameters  $\mu_L$ ,  $\mu_D$ ,  $\beta_L$ ,  $\beta_D$  and  $\tau$  of the bivariate lognormal distributions were calculated and are given in Table 2. When the impactor was used in the 3rd run, CML and CMD of inlet fibers were slightly smaller than those in the other runs, but there were clear decreases in both CML and CMD of deposited fibers compared to the 2nd run. In order to eliminate both large and small fibers, an impactor and a virtual impactor were used in the 4th run. As a result, although the geometric standard deviations  $\sigma_{g_L}$  and  $\sigma_{g_D}$  were not so small, large fibers were removed from fibrous aerosol flow, which is the same condition for all experiments. The values of CMD of inlet and deposited fibers were partly controllable by means of an impactor or the combination of an impactor and a virtual impactor, as pointed out by Burke and Esmen<sup>26)</sup> and Prodi *et al.*<sup>27)</sup>, who measured inertial behavior of fibrous aerosol.

*Deposited fractions as functions of fiber length and diameter*

The deposited fractions  $F_d$  in each range of fiber length

**Table 2. Parameters of bivariate lognormal distribution**

Run No.	1	2	3	4
Flow rate	15.6 cm <sup>3</sup> s <sup>-1</sup>	31.2 cm <sup>3</sup> s <sup>-1</sup>	31.2 cm <sup>3</sup> s <sup>-1</sup>	31.2 cm <sup>3</sup> s <sup>-1</sup>
Inlet fibers				
$\mu_L$	2.5	2.3	2.3	2.6
$\beta_L$	0.77	0.73	0.72	0.72
$\mu_D$	- 0.24	- 0.23	- 0.39	0.085
$\beta_D$	0.47	0.44	0.42	0.50
$\tau$	0.38	0.35	0.31	0.53
CML ( $\mu\text{m}$ )	11.9	10.1	10.2	13.9
$\sigma_{g_L}$	2.2	2.1	2.0	2.1
CMD ( $\mu\text{m}$ )	0.79	0.80	0.68	1.09
$\sigma_{g_D}$	1.6	1.5	1.5	1.7
Deposited fibers				
$\mu_L$	3.8	3.6	3.4	3.9
$\beta_L$	0.75	0.82	0.75	0.69
$\mu_D$	0.74	0.74	0.39	0.94
$\beta_D$	0.47	0.33	0.39	0.40
$\tau$	- 0.078	0.041	- 0.20	- 0.25
CML ( $\mu\text{m}$ )	44.0	36.8	28.6	51.0
$\sigma_{g_L}$	2.1	2.3	2.1	2.0
CMD ( $\mu\text{m}$ )	2.1	2.1	1.5	2.6
$\sigma_{g_D}$	1.6	1.4	1.5	1.5

**Table 3. Measured deposition fractions Fd for each length range**

Interception parameter		$2.4 \times 10^{-3}$		$4.7 \times 10^{-3}$		$9.4 \times 10^{-3}$		$1.46 \times 10^{-2}$	
Run No.	Length	Fd	Length	Fd	Length	Fd	Length	Fd	
1*	10–20 $\mu\text{m}$	$4.9 \times 10^{-4}$	20–40 $\mu\text{m}$	$1.6 \times 10^{-3}$	40–80 $\mu\text{m}$	$4.0 \times 10^{-3}$	70–110 $\mu\text{m}$	$6.3 \times 10^{-3}$	
2*	10–20 $\mu\text{m}$	$1.2 \times 10^{-3}$	20–40 $\mu\text{m}$	$5.7 \times 10^{-3}$	40–80 $\mu\text{m}$	$1.1 \times 10^{-2}$	70–110 $\mu\text{m}$	$2.2 \times 10^{-2}$	
3*	10–20 $\mu\text{m}$	$3.8 \times 10^{-4}$	20–40 $\mu\text{m}$	$2.0 \times 10^{-3}$	40–80 $\mu\text{m}$	$5.0 \times 10^{-3}$	70–110 $\mu\text{m}$	$8.9 \times 10^{-3}$	
4**	13–27 $\mu\text{m}$	$7.3 \times 10^{-4}$	27–53 $\mu\text{m}$	$3.1 \times 10^{-3}$	53–106 $\mu\text{m}$	$1.1 \times 10^{-2}$			

\*: Bifurcation model II was used in previous works. \*\*: Bifurcation model I was used in this work.

are shown in Table 3. Fd increases with both flow rate and fiber length. The data for the 4th run with the 2nd and 3rd model were newly obtained in this work.

The relationship between Stokes number and deposited fraction was reported in our previous work<sup>18,19</sup>. Fig. 2 shows the relationship between Stokes number and the deposited fraction calculated with  $\Delta D=0.1 \mu\text{m}$  in equation (3). In the figure, Stokes number St for randomly-oriented fibers<sup>2</sup>) is taken on the abscissa;

$$St = \frac{\rho D^2 U \sin \lambda}{16 \eta R \left[ \frac{0.385}{\ln(2L_f/D_f) - 0.5} + \frac{1.230}{\ln(2L_f/D_f) + 0.5} \right]} \quad (5)$$

For fibrous particles, Stokes number can be defined based on various equivalent diameters, since different fiber orientations in the flow field can be considered(i.e., parallel or perpendicular). In the calculation of St, the geometric mean fiber length  $L_f = \sqrt{L_1 \cdot L_2}$  is used in equation (5).

Fig. 2 shows that deposited fraction Fd sharply increases with both St and I. In particular, deposited fractions at small St, are strongly influenced by I, that is, the interception effect.

*Estimation of deposited fraction of fibers in the bifurcations*

The dimensionless relationship between St and Fd was used to estimate the deposited fraction at arbitrary positions at the upper bronchi. Since Fig. 2 reflects the effect of inertial impaction and interception of fibrous aerosol, one real curve of deposited fraction Fd for a given interception parameter I is expected to lie near the three or four lines for each range of I. Fig. 3 shows four curves of deposited fraction Fd for a given interception parameter  $I_n$ , which were obtained by fitting the experimental results in Fig. 3. In order to express these curves numerically, the following polynomial equation was employed,

$$F_{d_n} = \exp \{ a_{0_n} + a_{1_n} (\ln St) + a_{2_n} (\ln St)^2 + a_{3_n} (\ln St)^3 + a_{4_n} (\ln St)^4 \} \quad (6)$$

where  $n=1\sim 4$ . The sets of  $a_{0_n}$  to  $a_{4_n}$  at each interception

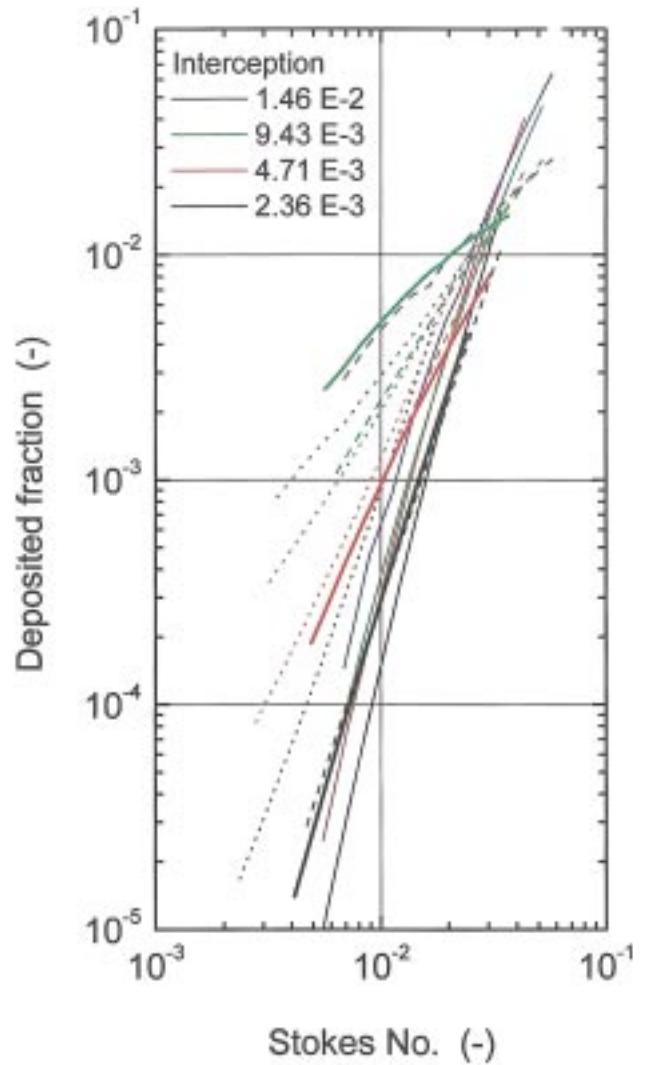


**Fig. 2. Relation between Stokes number for randomly-oriented fiber and deposited fraction.**

Bold lines in the figure indicate the results obtained from 4th run (this work). Other lines are referred to ref. (19)

**Table 4. Best-fit values of polynomial equations**

Interception parameter				
I	$2.4 \times 10^{-3}$	$4.7 \times 10^{-3}$	$9.4 \times 10^{-3}$	$1.46 \times 10^{-2}$
n	1	2	3	4
$a_0$	$0.55 \times 10$	$0.80 \times 10$	$0.98 \times 10$	$0.64 \times 10$
$a_1$	$0.27 \times 10$	$0.55 \times 10$	$0.69 \times 10$	$0.38 \times 10$
$a_2$	$-0.93 \times 10^{-2}$	$0.10 \times 10$	$0.12 \times 10$	0.15
$a_3$	$0.37 \times 10^{-1}$	0.17	0.14	$-0.38 \times 10^{-1}$
$a_4$	$0.64 \times 10^{-2}$	$0.12 \times 10^{-1}$	$0.72 \times 10^{-2}$	$-0.34 \times 10^{-2}$

$Fd_n = \exp\{a_0_n + a_1_n (\ln St) + a_2_n (\ln St)^2 + a_3_n (\ln St)^3 + a_4_n (\ln St)^4\}$  (6)  
 where  $n=1-4$ . The set of  $a_0_n$  to  $a_4_n$  at each interception parameter  $I_n$ .

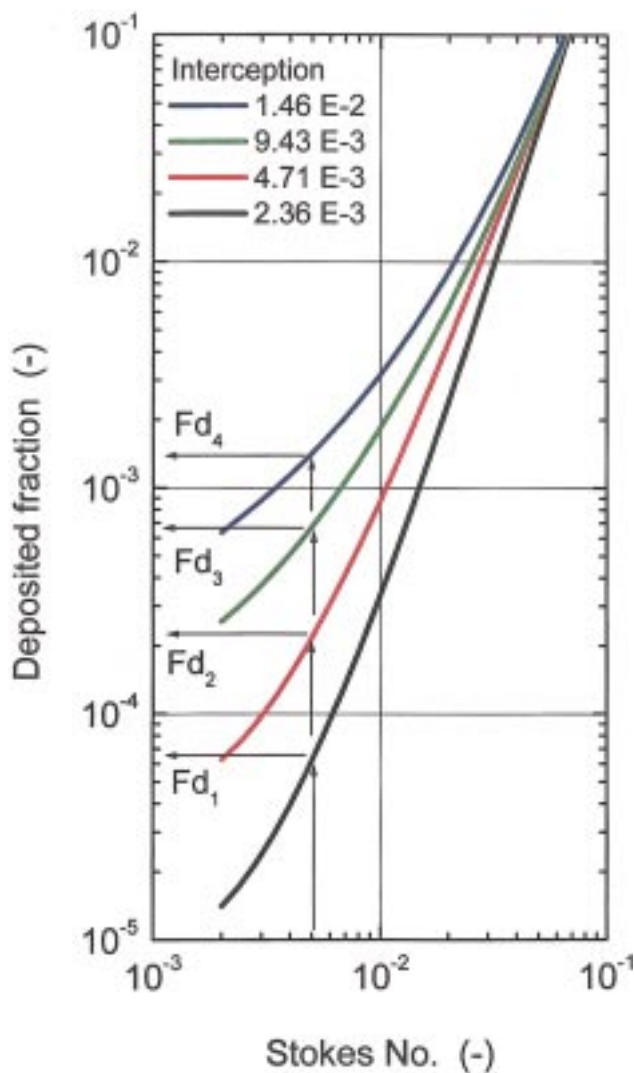


**Fig. 3. Visually fitted four curves on Fig.3 for each interception parameter I.**  
 For the estimation of Fd of arbitrary (St,I), four value of  $Fd_n$  ( $n=1-4$ ) are calculated as shown in the figure.

parameter  $I_n$  were determined by the least mean squares method and are given in Table 4.

The calculation procedure for  $Fd(St,I)$  consists of two steps: first the four deposited fractions  $Fd_n$  are determined by equation (6), as shown in Fig. 3. Then, Fd for I is obtained by interpolating or extrapolating the values of  $Fd_n$ . Fig. 4 shows the relationship between I and  $Fd_n$  for five Stokes numbers. In the figure the Fd shows a linear relation with I. From four values of ( $I_n, Fd_n$ ), a and b in the following equation were determined by means of the least mean squares method.

$$Fd(St,I) = a I^b \tag{7}$$

With this procedure, it is possible to determine the deposited

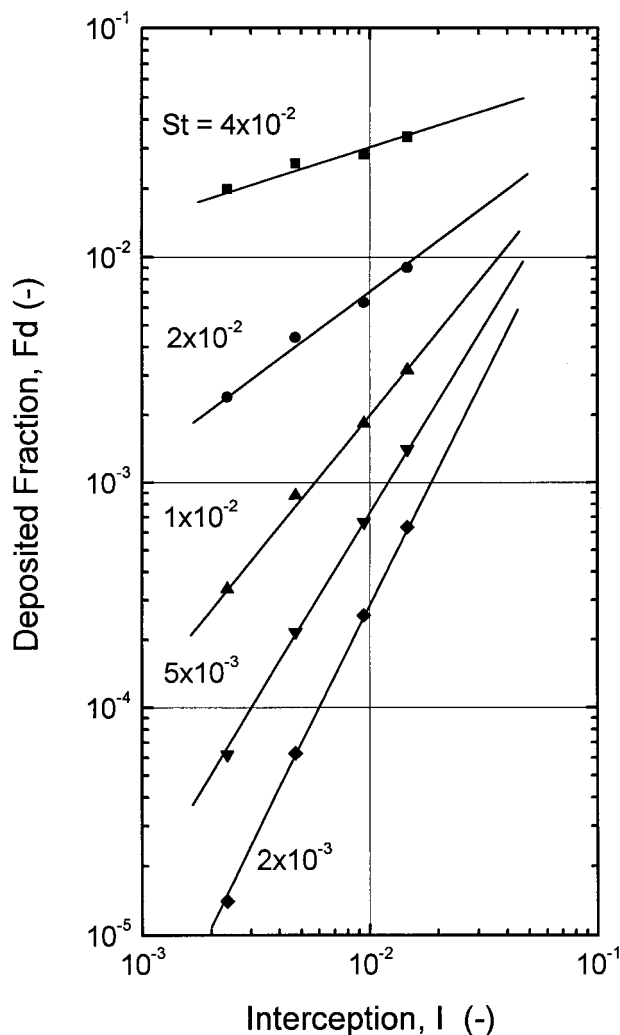


**Fig. 4. Relation between interception parameter I and deposited fraction obtained from Fig. 3.**  
 For the estimation of Fd of arbitrary I, four value of  $Fd_n$  ( $n=1-4$ ) used to interpolation or extrapolation.

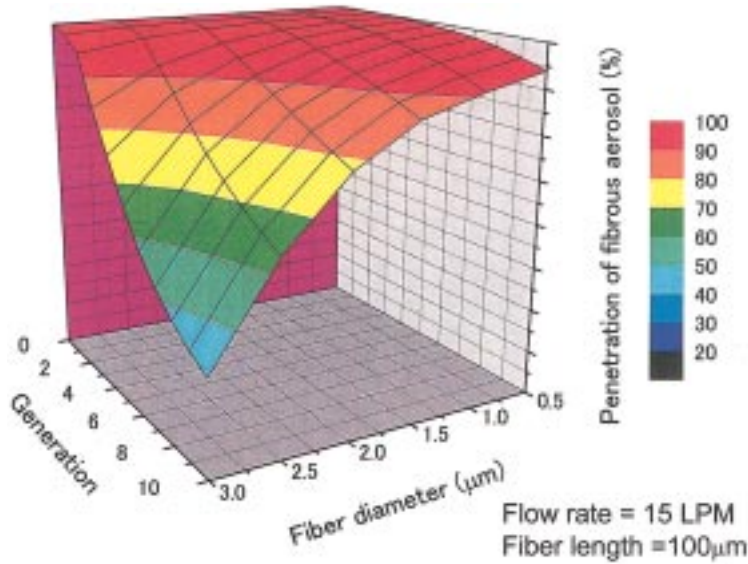


**Fig. 5. Estimated penetration of airborne fibers through trachea to 10 generation.**

Fiber length is  $100 \mu\text{m}$  and fiber diameter is from  $0.5$  to  $3.0 \mu\text{m}$ . All branch angle of bifurcation is assumed to be  $45^\circ$ .

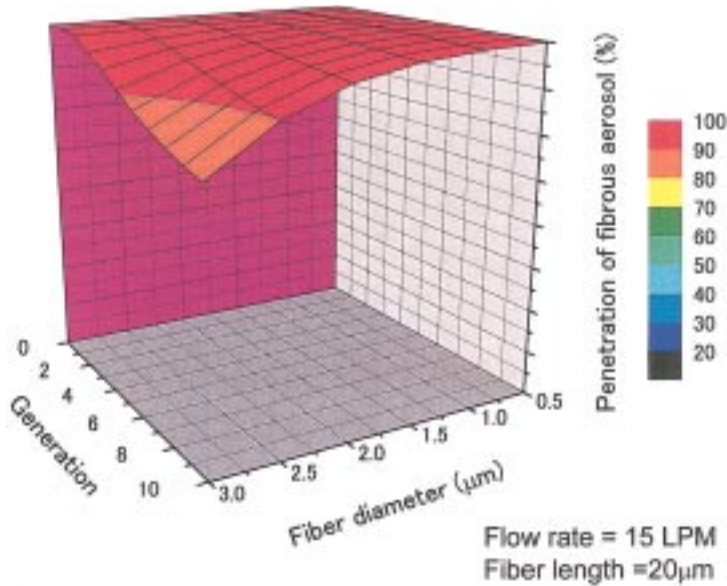


**Fig. 6. Estimated penetration of airborne fibers through trachea to 10 generation.**

Fiber length is  $20 \mu\text{m}$  and fiber diameter is from  $0.5$  to  $3.0 \mu\text{m}$ . All branch angle of bifurcation is assumed to be  $45^\circ$ .

fraction  $F_d$  in the range of  $2 \times 10^{-3} < St < 5 \times 10^{-2}$  and  $5 \times 10^{-4} < I < 5 \times 10^{-2}$ .

#### *Penetration of fibrous aerosol in the upper bronchi*

Penetration from the trachea to the 10th generation of lung bifurcation with dimensions based on symmetric model A of Weibel was calculated for several fiber diameters, lengths and flow rates. Fig.5 shows the estimated penetration of fibrous aerosol at each bifurcation for the fibers with a length of  $100 \mu\text{m}$  and a diameter of  $0.5$  to  $3.0 \mu\text{m}$ . Penetration through  $m$ -th bifurcation is given by

$$P_m = P_{m-1} (1 - F_{d_m}) \quad (8)$$

where  $m=1 \sim 10$ . The generation of the trachea is 0 and  $P_0=100$ . One color in the figure indicates 10% change in penetration. This figure corresponds to an inspiration of  $500 \text{ cm}^3$  air at a constant rate for 2 s. More than half of the fibers with a length of  $100 \mu\text{m}$  and diameter of  $3 \mu\text{m}$  are deposited at upper bronchi but more than 90% of fibers which have the same length and  $1 \mu\text{m}$  in diameter pass through the region.

Fig. 6 shows the estimated change in fibrous aerosol penetration in each bifurcation for a fiber length of  $20 \mu\text{m}$ . Other parameters are the same as in Fig. 5. Only 20% of fibers with a diameter of  $3 \mu\text{m}$  are deposited at upper bronchi.

The deposited fractions of randomly-oriented fibers by

impaction and interception were calculated from a theoretical equation by Harris and Fraser<sup>2</sup>). Although the calculated deposited fraction increased with St, their dependencies on St and I are less than our results<sup>19</sup>).

The values for deposited fractions presented in this work should be much larger because the deposited fibers were measured only on the wall of the daughter tube from the carina to 4 or 6 mm downstream. Although fewer fibers were deposited further downstream, compared to fibers deposited at carinal region, they were not negligible<sup>17</sup>). Furthermore, the deposited fractions increased at cyclic flow conditions. Previous data<sup>18</sup>) suggested that the deposited fractions at 30 breaths min<sup>-1</sup> were 1.4–1.7 times greater than those at steady flow with the same time-averaged flow rate. Therefore, it is conceivable that twice or more of fibers may deposit at each bifurcation.

Our estimation method based on experimental data provides a way to calculate the deposited fraction of airborne fibers at upper bronchi by the effects of inertia and interception. The model predicts that almost all of fine fibers, of which the diameter is less than 1  $\mu\text{m}$ , pass through the upper bronchi and enter the alveolar region.

## Acknowledgements

The authors greatly appreciate Dr. Yoshio Otani (Kanazawa University) for his suggestions and assistance in editing the text of this paper.

## References

- 1) Beekman JM (1972) Deposition of ellipsoidal particles in the human respiratory tract. In: Assessment of airborne particles eds. by Mercer TT, Morrow PE, Stober W, 361–70, Springfield, Illinois.
- 2) Harris RL, Fraser DA (1976) A model for deposition of fibers in the human respiratory system. *Am Ind Hyg Assoc J* **37**, 73–89.
- 3) Harris RL, Timbrell V (1977) The influence of fibre shape in lung deposition-mathematical estimates. In: Inhaled particles IV eds. by Walton WH, 75–89. Pergamon Press, Oxford.
- 4) Yu CP, Asgharian B, Yen BM (1986) Impaction and sedimentation deposition of fibers in airways. *Am Ind Hyg Ass J* **47**, 72–7.
- 5) Yu CP, Asgharian B, Pinkerton KE (1991) Intrapulmonary deposition and retention modeling of chrysotile asbestos fibers in rats. *J Aerosol Sci* **22**, 757–63.
- 6) Yu CP, Zhang L, Oberdorster GO, Mast RW, Glass LR, Utell MJ (1994) Deposition modeling of refractory ceramic fibers in the rat lung. *J Aerosol Sci* **25**, 407–17.
- 7) Yu CP, Zhang L, Oberdorster GO, Mast RW, Maxim D, Utell MJ (1995) Deposition of refractory ceramic fibers in the human respiratory tract and comparison with rodent studies. *Aerosol Sci Technol* **23**, 291–300.
- 8) Cai FS, Yu CP (1988) Inertial and interceptional deposition of spherical particles and fibers in a bifurcating airway. *J Aerosol Sci* **19**, 679–88.
- 9) Asgharian B, Yu CP (1988) Deposition of inhaled fibrous particles in the human lung. *J Aerosol Med* **1**, 37–50.
- 10) Asgharian B, Yu CP (1989) Deposition of fibers in the rat lung. *J Aerosol Sci* **20**, 355–66.
- 11) Chen YK, Yu CP (1991) Sedimentation of charged fibers from a circular duct flow. *J Aerosol Sci* **22**, 747–56.
- 12) Ding JY, Yu CP, Zhang L, Chen YK (1997) Deposition modeling of fibrous particles in rats: Comparisons with available experimental data. *Aerosol Sci Technol* **26**, 403–14.
- 13) Dai YT, Yu CP (1998) Alveolar deposition of fibers in rodents and humans. *J Aerosol Med* **11**, 247–58.
- 14) Timbrell V (1972) Inhalation and biological effects of asbestos. In: Assessment of airborne particles eds. by Mercer TT, Morrow PE, Stober W, 429–45, Springfield, Illinois.
- 15) Petra AL (1979) An experimental study on deposition of chrysotile asbestos fibers in human lung model. Ph. D. Thesis. North Carolina State University.
- 16) Kahn RA (1982) A method for investigating the deposition of fibers and spheres at the carina in excised lungs. Ph. D. Thesis. University of Pittsburgh.
- 17) Myojo T (1987) Deposition of fibrous aerosol in model bifurcating tubes. *J Aerosol Sci* **18**, 337–47.
- 18) Myojo T (1989) Deposition of fibrous aerosol in a model of a human lung bifurcation under cyclic flow conditions. *J Aerosol Res, Japan* **4**, 198–205 (in Japanese).
- 19) Myojo T (1990) The effect of length and diameter on the deposition of fibrous aerosol in a model lung bifurcation. *J Aerosol Sci* **21**, 651–9.
- 20) Myojo T (1997) Deposition of fibrous aerosol in a model of a human lung bifurcation under cyclic flow conditions. *Ann Occup Hyg Supplement 1* **41**, 142–7.
- 21) Weibel ER (1963) *Morphometry of the Human Lung*, Springer, Berlin.

- 22) Timbrell V (1982) Deposition and retention of fibres in the human lung. *Ann Occup Hyg* **26**, 347–69.
- 23) Schneider T, Holst E (1983) Man-made mineral fibre size distributions utilizing unbiased and fibre length biased counting methods and the bivariate log-normal distribution. *J Aerosol Sci* **14**, 139–46.
- 24) Cheng YS (1986) Bivariate lognormal distribution for characterizing asbestos fiber aerosols. *Aerosol Sci Technol* **5**, 359–68.
- 25) Myojo T (1983) A fibrous aerosol generator using a two-component fluidized bed. *Ind Health* **21**, 79–89.
- 26) Burke WA, Esmen N (1978) The inertial behavior of fibers. *Am Ind Hyg Assoc J* **39**, 400–5.
- 27) Prodi V, Zaiacomo T De, Hochrainer D, Spurny K (1982) Fibre collection and measurement with the inertial spectrometer. *J Aerosol Sci* **13**, 49–58.